Plakophilin-2 loss promotes TGF-β1/p38 MAPK-dependent fibrotic gene expression in cardiomyocytes

Adi D. Dubash,[1,3]* Chen Y. Kam,[1]* Brian A. Aguado,[4,6] Dipal M. Patel,[1] Mario Delmar,[7] Lonnie D. Shea,[5,8] and Kathleen J. Green[1,2]

[1]Department of Pathology and [2]Department of Dermatology, Northwestern University Feinberg School of Medicine, Chicago, IL 60611
[3]Department of Biology, Furman University, Greenville SC 29613
[4]Department of Biomedical Engineering, Northwestern University, Evanston IL 60208
[5]Department of Chemical and Biological Engineering, Northwestern University, Evanston, IL 60208
[6]Simpson Querrey Institute for BioNanotechnology, Northwestern University, Chicago IL 60611
[7]New York University School of Medicine, New York, NY 10016
[8]Department of Biomedical Engineering, University of Michigan, Ann Arbor, MI 48105

Members of the desmosome protein family are integral components of the cardiac *area composita*, a mixed junctional complex responsible for electromechanical coupling between cardiomyocytes. In this study, we provide evidence that loss of the desmosomal armadillo protein Plakophilin-2 (PKP2) in cardiomyocytes elevates transforming growth factor β1 (TGF-β1) and p38 mitogen-activated protein kinase (MAPK) signaling, which together coordinate a transcriptional program that results in increased expression of profibrotic genes. Importantly, we demonstrate that expression of Desmoplakin (DP) is lost upon PKP2 knockdown and that restoration of DP expression rescues the activation of this TGF-β1/p38 MAPK transcriptional cascade. Tissues from PKP2 heterozygous and DP conditional knockout mouse models also exhibit elevated TGF-β1/p38 MAPK signaling and induction of fibrotic gene expression in vivo. These data therefore identify PKP2 and DP as central players in coordination of desmosome-dependent TGF-β1/p38 MAPK signaling in cardiomyocytes, pathways known to play a role in different types of cardiac disease, such as arrhythmogenic or hypertrophic cardiomyopathy.

Introduction

Vertebrate cardiac myocytes are coupled to each other by a mixed or hybrid cell–cell junction complex known as the *area composita*, comprising adherens junctions (AJs), desmosome (DSM) proteins, and associated gap junctions (Borrmann et al., 2006; Delmar and McKenna, 2010). DSM proteins from three different families are present in the *area composita* in cardiomyocytes (CMs; Green and Simpson, 2007; Delmar and McKenna, 2010). The transmembrane cadherins Desmoglein-2 and Desmocollin-2 physically link together in the extracellular space by calcium-dependent interactions. The desmosomal armadillo protein Plakophilin-2 (PKP2) binds to other catenin proteins in the complex, such as γ-catenin/plakoglobin (PG) and αT-catenin, and serves as a link to the cytoskeletal linker protein Desmoplakin (DP), which attaches the complex to the desmin intermediate filament network (Goossens et al., 2007; Green and Simpson, 2007; Delmar and McKenna, 2010).

PKP2 has a well-established role in maintaining the organization of DSMs, including the recruitment and stabilization of DP into cell–cell junctions (Bass-Zubek et al., 2008; Godsel et al., 2010). Because it is the only plakophilin expressed in cardiac cells (Gandjbakhch et al., 2011), loss of PKP2 disrupts normal *area composita* formation (Pieperhoff et al., 2008). PKP2 knockout mice die during embryogenesis at embryonic day (E) 11.5 because of major defects in cardiac development, and analysis of the intercalated disk at E10.75 demonstrated significant defects in *area composita* formation (Grossmann et al., 2004). In addition to decreased mechanical stability, loss of PKP2 causes mislocalization of Connexin43, disruption of gap junctions, and decreased sodium current, highlighting the interdependence between mechanical and electrical coupling in normal CMs (Oxford et al., 2007; Sato et al., 2009). Mutation of PKP2 is a common occurrence in arrhythmogenic cardiomyopathy (AC), a disorder characterized by disruption of cardiac electromechanical junctions and replacement of healthy CMs with fibrous and fatty tissue (Syrris et al., 2006; Delmar and McKenna, 2010). While these data point to an important role for PKP2 in regulating mechanical stability of tissues, recent studies have highlighted PKP2's multifaceted functions in regulating

---

*A.D. Dubash and C.Y. Kam contributed equally to this paper.

Correspondence to Kathleen J. Green: kgreen@northwestern.edu

Abbreviations used in this paper: AC, arrhythmogenic cardiomyopathy; AJ, adherens junction; CF, cardiac fibroblast; CM, cardiomyocyte; DP, Desmoplakin; DSM, desmosome; E, embryonic day; FN, fibronectin; MKK, MAPK kinase; NHEK, normal human epidermal keratinocyte; PG, Plakoglobin; PKP2, plakophilin-2; qPCR, quantitative real-time PCR; TAK1, TGF-β–associated kinase 1.

different DSM-dependent signaling pathways (Bass-Zubek et al., 2009; Chen et al., 2014; Munoz et al., 2014). Importantly, loss of PKP2 suppresses β-catenin/YAP signaling, leading to an up-regulation of adipogenic gene expression in CMs (Chen et al., 2014). In this study, we identify a novel role for PKP2 in coordination of a TGF-β1/p38 MAPK signaling cascade that results in activation of a profibrotic transcriptional program. Loss of PKP2 in neonatal CMs increases expression of TGF-β1, a potent profibrotic cytokine (Leask, 2007). In response to elevated TGF-β1, activation of the p38 MAPK signaling cascade coordinates a transcriptional program, leading to increased expression of both inflammatory and fibrotic genes in CMs.

Activation of TGF-β1/p38 MAPK signaling is dependent on loss of DP expression because restoration of DP expression in a PKP2 knockdown (KD) background was sufficient to rescue the induction of this signaling cascade. These data are recapitulated in vivo, as demonstrated by an increase in TGF-β1 mRNA levels, p38 MAPK activation, and fibrotic gene expression in tissue samples from PKP2 heterozygous mice and a DP conditional knockout mouse model. These data therefore identify a novel role for the DSM proteins PKP2 and DP in coordinating TGF-β1/p38 MAPK profibrotic signaling. In different types of heart disease, excessive ECM gene expression leads to fibrosis, a deleterious process leading to stiffness, scar formation, and CM atrophy (Jellis et al., 2010; Krenning et al., 2010; Weber et al., 2013). These findings have broad implications for the study of cardiac disease involving both mutation of DSM proteins (e.g., AC) and profibrotic transcriptional pathways (e.g., dilated/hypertrophic cardiomyopathy).

Results

Loss of PKP2 disrupts *area composita* formation via loss of DP localization and stability

To uncover the molecular mechanisms behind the up-regulation of profibrotic signaling in cardiac myocytes, we used a well-established cellular model system of cultured neonatal rat ventricular CMs. This cellular model has been used successfully to investigate altered signaling pathways in cardiac disease, and parallel studies with transgenic mouse models have demonstrated consistent findings between the two approaches (Garcia-Gras et al., 2006; Yang et al., 2006). Freshly isolated CMs were infected with adenovirus containing either control or PKP2 KD constructs, and samples were analyzed 72 h post-infection. PKP2 is required for maintenance of structural integrity of cardiac cell–cell junctions, and previous studies have characterized the disruption of specific junctional components on loss of PKP2 (Grossmann et al., 2004). To confirm these results in our model, we analyzed the localization of DSM and AJ proteins upon PKP2 KD in CMs. PKP2 KD was confirmed by loss of PKP2 staining at cell–cell junctions (Fig. 1 A) and also by analysis of protein levels by Western blot (Fig. 1 B). As expected from studies in other cell types, PKP2 KD resulted in an almost complete loss from cell borders of the cytoskeletal linker protein DP, a close binding partner of PKP2. In addition, as previously described, loss of PKP2 also caused a reduction in junctional Cnx43 staining (Fidler et al., 2009; Sato et al., 2009). Importantly, loss of PKP2 did not disrupt localization of AJ components because staining for β-catenin and p120-catenin was not changed upon PKP2 KD. Junctional localization of PG, the other DSM armadillo protein expressed in CMs, was not

majorly perturbed, and its protein expression levels were not changed between control and PKP2 KD cells (Fig. 1, A and B).

The protein expression levels of other DSM and AJ proteins were also not affected by loss of PKP2, with one major exception. Surprisingly, in addition to loss of junctional localization, DP protein expression was reduced by 60–70% in PKP2 KD CMs (Fig. 1 B). Previous studies in epithelial cells have demonstrated that although PKP2 KD causes a reduction of DP border localization, its expression levels are not affected (Bass-Zubek et al., 2008; Godsel et al., 2010). These data therefore indicate an additional, previously unappreciated level of regulation of DP by PKP2 that is unique to CMs.

To validate that the observed reduction in DP protein was caused specifically by loss of PKP2, we re-expressed V5-tagged PKP2 in a PKP2 KD background. Ectopically expressed PKP2 restored the DP protein levels in these cells (Fig. 1 C). Further, we analyzed the solubility of DP by performing a Triton fractionation assay. In control cells, DP's association with PKP2 facilitated its cortical recruitment and proper incorporation into Triton-insoluble DSMs. PKP2 KD resulted in an increase in the amount of DP in the Triton-soluble fraction, consistent with the idea that impairing DP's normal attachment to DSMs destabilizes the protein (Fig. 1 D). We also observed an increase in the amount of the intermediate filament protein desmin in the soluble fraction, giving further support to the hypothesis that stability of DP in cell–cell junctions is compromised on loss of PKP2 (Fig. 1 D).

To investigate the mechanism via which PKP2 regulates DP expression levels in CMs, we first analyzed the levels of *Dsp* mRNA. Loss of PKP2 did not reduce *Dsp* mRNA levels, indicating that a transcriptional mechanism for regulating DP expression is not involved (Fig. 1 E). We therefore analyzed DP protein stability by treating cells with cycloheximide for the indicated time points. The rate of degradation of DP upon PKP2 KD was increased compared with control (Fig. 1 F). Further, the loss of DP expression observed in PKP2 KD cells was rescued by treatment with a proteasomal inhibitor (MG132), but not a lysosomal inhibitor (chloroquine; Fig. 1 G). Collectively, these data demonstrate that PKP2 is critical for the stable incorporation of DP into cell–cell junctions, loss of which causes an increase in DP solubility and subsequent degradation by the proteasome.

PKP2 loss triggers an increase in TGF-β1 expression and transcriptional signaling

In addition to its adhesive functions, PKP2 has been shown to coordinate the activity of different signaling pathways. A common characteristic of AC is the replacement of healthy myocardium with fibro-fatty deposits. We therefore asked whether loss of PKP2 in CMs triggers profibrotic signaling responses. TGF-β is a well-known agonist of fibrotic signaling pathways and has been shown to regulate the expression of ECM proteins in multiple studies (Leask, 2007, 2010; Dobaczewski and Frangogiannis, 2009; Dobaczewski et al., 2011). Determination of TGF-β mRNA levels by quantitative real-time PCR (qPCR) revealed a significant increase in the levels of *Tgfb1*, but not *Tgfb2* or *Tgfb3* mRNA (Fig. 2 A). In addition, we detected a significant increase in TGF-β1 levels in the supernatant of cultured PKP2 KD CMs compared with controls, indicating that loss of PKP2 in neonatal CMs induces an increase in levels of secreted TGF-β1 (Fig. 2 B). To determine whether loss of PKP2 results in elevated TGF-β1 signaling in vivo, we used a PKP2$^{+/−}$ mouse model (Grossmann et al., 2004; Cerrone et al., 2012). Analysis of total mRNA extracts from samples of mouse hearts showed
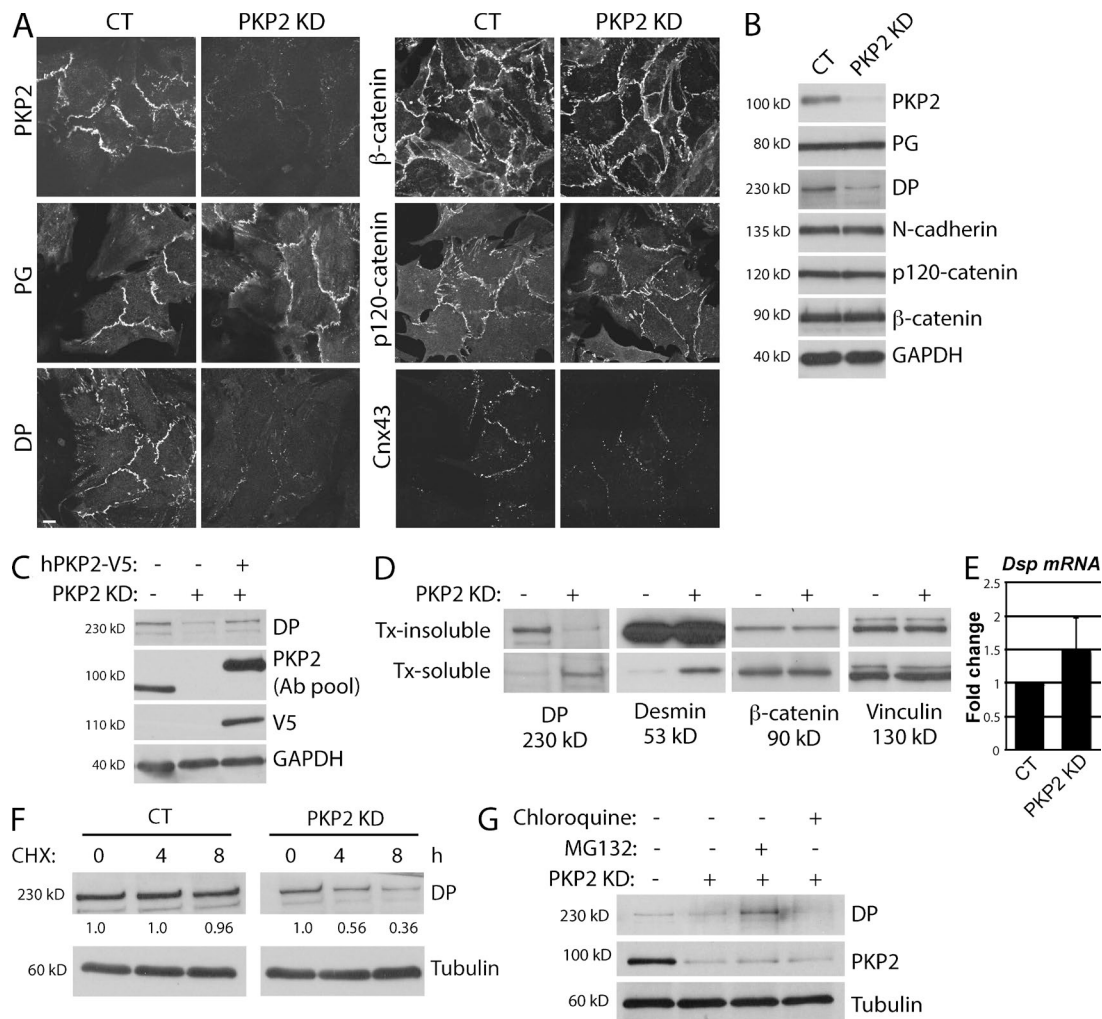
Figure 1. **PKP2 KD in neonatal CMs disrupts *area composita* formation via loss of DP localization and stability.** Freshly isolated neonatal CMs were infected with adenovirus containing either control or PKP2 KD constructs, and samples were analyzed 72 h postinfection. (A) Control (CT) and PKP2 KD CMs grown on coverslips were stained for cell–cell junction components, including PKP2, PG, DP, β-catenin, p120-catenin, and Cnx43. PKP2 KD specifically results in a major loss of DP and Cnx43 from junctions, but not other junctional markers. Bar, 20 μm. (B) Protein levels of cell–cell junction proteins are not perturbed on loss of PKP2, except DP, whose expression is reduced by 60–70%. (C) Re-expression of human V5-tagged PKP2 in rat PKP2 KD CMs rescues DP protein levels. A pool of two antibodies was used to analyze PKP2 levels in this experiment (described in Materials and methods). (D) PKP2 KD results in an increase in DP solubility, as indicated by a decrease in DP levels in the Triton X-100 (Tx)–insoluble fraction and a concomitant increase in the Triton X-100–soluble fraction. Solubility of the intermediate filament protein Desmin is also increased, but solubility of other junctional markers such as β-catenin is not affected. Vinculin is included as a loading control. (E) RNA extracted from control and PKP2 KD cells was analyzed for *Dsp* mRNA levels by qPCR. Transcription of DP is not decreased on loss of PKP2 KD in CMs. (F) Control and PKP2 KD cells were treated with cycloheximide (CHX) for the indicated times, and samples are blotted for DP and tubulin. Degradation of DP is increased in PKP2 KD cells compared with control, as indicated by quantification of DP band intensity (normalized to tubulin) at the various time points. All images and blots shown are representative of three independent experiments. (G) Control, PKP2 KD, and PKP2 KD CMs treated with either a proteasomal inhibitor (MG132) or a lysosomal inhibitor (chloroquine) were blotted for DP and tubulin (loading control). DP expression in PKP2 KD cells was restored by proteasomal inhibition, but not lysosomal inhibition.

that haploinsufficiency of PKP2 is sufficient to significantly increase *Tgfb1* mRNA levels compared with controls (Fig. 2 C).

The canonical TGF-β signaling pathway involves binding of TGF-β ligands to a complex of TGF-β type I and II receptors and activation of receptor-SMADS 2 and 3, which activate transcription of target genes (Massagué et al., 2005). To determine if increased TGF-β1 expression by CMs results in activation of canonical SMAD signaling, we used a SMAD luciferase reporter assay in conjunction with noninvasive imaging to analyze luciferase expression in the same cells over a period of 6 d (Bellis et al., 2013; Siletz et al., 2013; Aguado et al., 2015). Luciferase activity after KD demonstrated a significant increase in SMAD3 activation in PKP2 KD CMs (Fig. 2 D). Loss of PKP2 also resulted in the activation of the transcription factors STAT3 and NF-κB in

CMs (Fig. 2, E and F; Haghikia et al., 2011, 2014). The activity of other transcription factors (e.g., AP1 and MEF2) was not dramatically perturbed, highlighting the specificity in the transcriptional response induced by TGF-β1 in PKP2 KD cells (Fig. S1).

Up-regulation of TGF-β1 in PKP2-KD CMs activates a p38 MAPK signaling cascade

We next investigated the mechanism by which loss of PKP2 induces activation of TGF-β–dependent transcription. It has been shown that TGF-β can signal to p38 MAPK via TGF-β–associated kinase 1 (TAK1; a MAPK kinase [MKK] kinase) and MKK3/6 during myocardial infarction in rats (Zhang et al., 2000; Matsumoto-Ida et al., 2006). The TAK1–MKK3–p38 MAPK cascade is known to be important for TGF-β–induced collagen
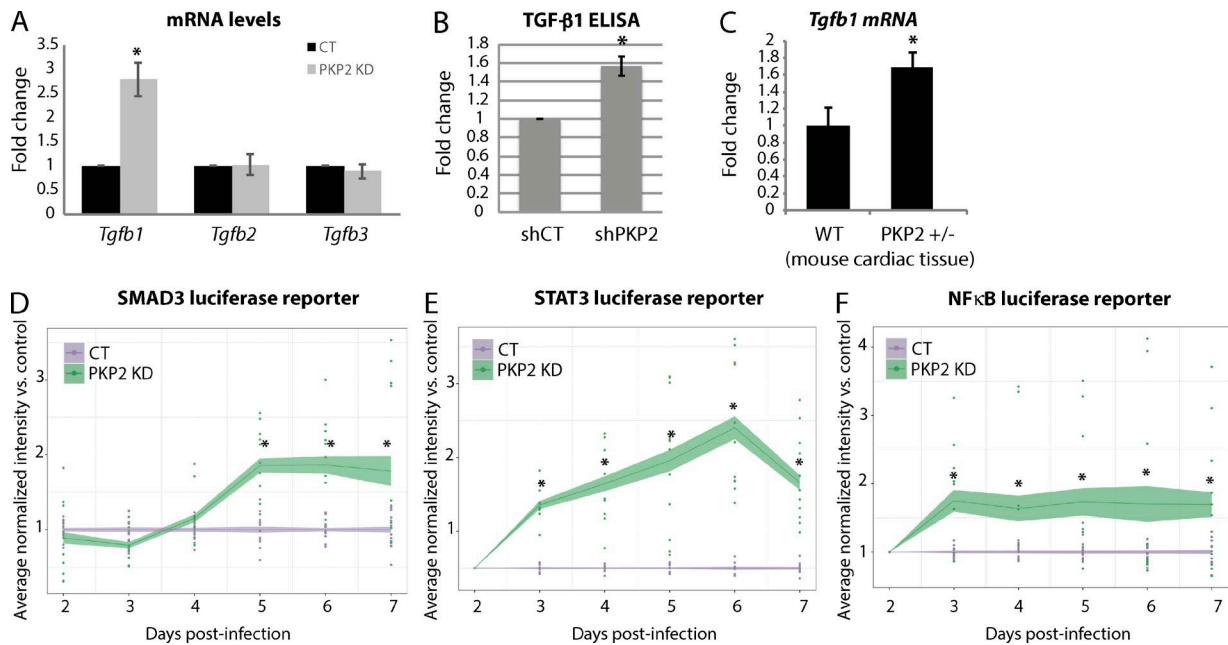
Figure 2. **PKP2 loss triggers an increase in TGF-β1 expression and transcriptional signaling.** (A) RNA isolated from control (CT) and PKP2 KD CMs were analyzed for mRNA levels of the TGF-β genes. *Tgfb1* (but not *Tgfb2* or *Tgfb3*) mRNA levels were significantly increased on KD of PKP2. (B). Levels of TGF-β1 were analyzed in the cell culture supernatants of control and PKP2 KD cells 72 h after KD by performing a TGF-β1 ELISA. These data indicate a significant increase in secreted TGF-β1 on loss of PKP2. (C) RNA isolated from wild-type and PKP2^+/− mouse heart tissue were analyzed for mRNA levels of *Tgfb1*. Haploinsufficiency of PKP2 results in a significant increase in *Tgfb1* mRNA in vivo. (D–F) SMAD3, STAT3, and NF-κB transcriptional activity was followed via luciferase reporter arrays (see Materials and methods). After control and PKP2 KD in 96-well plates, CMs were infected with luciferase reporter constructs for SMAD3, STAT3, or NF-κB and luciferase expression followed in the same cells by noninvasive imaging for a period of 6 d. KD of PKP2 caused a significant increase in transcriptional activity of SMAD3, STAT3, and NF-κB. For all graphs, fold change values from three independent samples are represented with error bars indicating SD. *, P < 0.05.

production (Ono et al., 2003; Kim et al., 2007). Loss of PKP2 in CMs increased the activity of sequential members of this MAPK cascade, TAK1, MKK3/6, and p38 MAPK (Fig. 3 A). Up-regulation of this MAPK cascade (and loss of DP expression) was recapitulated both in PKP2^+/− mouse hearts (Fig. 3 B) and upon PKP2 KD in the HL-1 cardiomyocyte cell line (Fig. 3 C).

Activation of p38 MAPK signaling was confirmed by immunofluorescence, which revealed a marked increase in nuclear accumulation of phosphorylated (active) p38 MAPK in PKP2 KD CMs compared with controls (Fig. 3 D). In the PKP2 KD condition (but not in the control), we observed that a small percentage of cells not expressing the PKP2 KD construct (as indicated by lack of GFP expression) also displayed elevated levels of phospho–p38 MAPK (Fig. S2 A). These data indicate that PKP2 KD can induce p38 MAPK activation in a non–cell-autonomous fashion. Further, because isolations of CMs from neonatal hearts can be contaminated with neonatal fibroblasts, we costained cells with the CM-specific marker desmin. Nuclear phospho–p38 MAPK staining was clearly seen in desmin-stained CMs, indicating that activation of p38 MAPK occurs in CMs (Fig. S2 B). Additionally, active p38 MAPK was rescued on re-expression of PKP2-V5, confirming that this effect is specific to PKP2 (Fig. 3 E).

Activation of the p38 MAPK signaling cascade in PKP2 KD CMs is dependent on TGF-β signaling

We next sought to validate the sequential events in this signaling pathway by confirming that activation of p38 MAPK is induced by TGF-β signaling. To do this, we used inhibitors to TGF-β1 receptor I and TAK1. Inhibition of either TGF-β1 receptor I (with SB431542) or TAK1 [with (5Z)-7-Oxozeaenol] rescued the elevation of MKK3/6 and p38 MAPK phosphorylation seen on loss of PKP2 (Fig. 4, A and B). Because p38 MAPK signaling has been shown to promote activation of some cytokines, we asked whether the observed increase in TGF-β1 expression might be a result of p38 MAPK activation. Treatment of CMs with the p38 MAPK inhibitor SB203580 in a PKP2 KD background did not restore *Tgfb1* mRNA levels, indicating that this effect is upstream of p38 MAPK activation (Fig. 4 C). In support of these data, stimulation of normal CMs with TGF-β1 ligand was sufficient to elevate phosphorylation of both MKK3/6 and p38 MAPK (Fig. 4 D). These data establish the autocrine activation of a TAK1–MKK3/6–p38 MAPK cascade in response to TGF-β1 up-regulation in PKP2 KD CMs.

Loss of PKP2 induces inflammatory and fibrotic gene expression in CMs

The evidence that p38 MAPK plays a role in cardiac fibrosis comes from studies showing that activation of p38 MAPK signaling in rat hearts resulted in increased inflammation and fibrosis. Importantly, global gene expression studies indicated that profibrotic inflammatory mediators were significantly up-regulated in p38 MAPK activated hearts (Clerk and Sugden, 2006; Tenhunen et al., 2006). We therefore next investigated the consequences of increased p38 MAPK activity in PKP2 KD CMs. Loss of PKP2 resulted in a significant increase in mRNA expression of interleukin-1α (*Il1a*) and *Ccl12*, both of which have been shown to have profibrotic
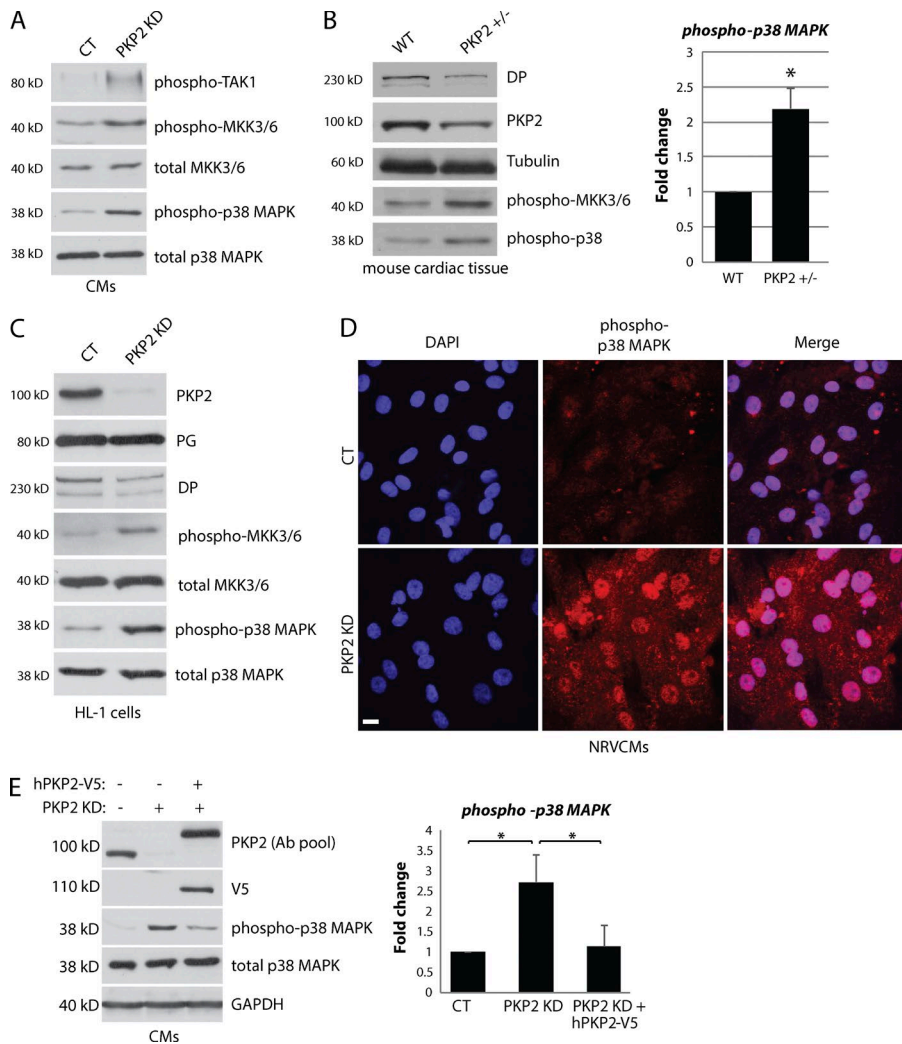
Figure 3. **PKP2 KD results in activation of a p38 MAPK signaling cascade.** (A) Control (CT) and PKP2 KD CMs were blotted for phosphorylated forms of TAK1, MKK3/6, and p38 MAPK, all of which are increased on loss of PKP2. (B) Wild-type (WT) and PKP2$^{+/-}$ mouse heart samples were lysed and blotted for DP, PKP2, tubulin, and phosphorylated forms of MKK3/6 and p38 MAPK. Loss of PKP2 expression results in activation of p38 MAPK in vivo, quantified in the graph (right). (C) KD of PKP2 in the HL1 cardiomyocyte cell line recapitulates these results, showing an increase in phospho-MKK3/6 and phospho–p38 MAPK compared with controls. Loss of DP expression is also demonstrated in this cell line. (D) Freshly isolated cultures of control and PKP2 KD CMs grown on coverslips were stained for phospho–p38 MAPK. These data indicate an increase in nuclear staining of phospho–p38 MAPK on loss of PKP2. Bar, 20 µm. (E). Re-expression of human V5-tagged PKP2 in rat PKP2 KD CMs rescues the increase in phospho–p38 MAPK. A pool of two antibodies was used to analyze PKP2 levels in this experiment (described in Materials and methods). Quantification of these results across multiple experiments are shown in the graph (right). For all graphs, fold change values from three independent samples are represented with error bars indicating SD. *, $P < 0.05$. NRVCM, neonatal rat ventricular CM.
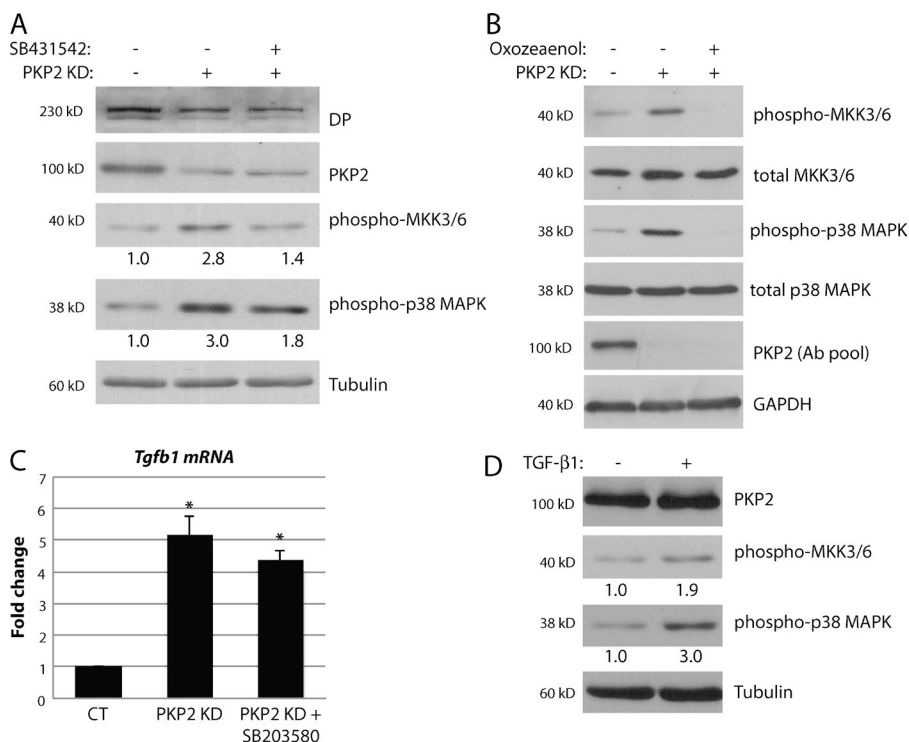
Figure 4. **Activation of p38 MAPK in PKP2 KD CMs occurs via up-regulation of TGF-β1 signaling.** (A and B) Control (CT), PKP2 KD, and PKP2 KD CMs treated with either a TGFβR1 inhibitor (SB431542) (A) or a TAK1 inhibitor [(5Z)-7-Oxozeaenol] (B) were blotted for phosphorylated forms of MKK3/6 and p38 MAPK. Inhibition of either TGFβR1 or TAK1 abrogates the activation of the downstream kinases MKK 3/6 and p38 MAPK seen on loss of PKP2. (C) *Tgfb1* mRNA levels are analyzed in control, PKP2 KD, and PKP2 KD cells treated with the p38 MAPK inhibitor SB203580. The increase in *Tgfb1* mRNA levels is not abrogated by inhibition of p38 MAPK. (D) Normal CMs were treated with TGF-β1 ligand for 4 h, lysed, and blotted for phosphorylated forms of MKK3/6 and p38 MAPK. These data indicate that stimulation of CMs with TGF-β1 is sufficient to induce activation of the p38 MAPK pathway in CMs. All images and blots shown are representative of three independent experiments. For all graphs, fold change values from three independent samples are represented with error bars indicating SD. *, $P < 0.05$.
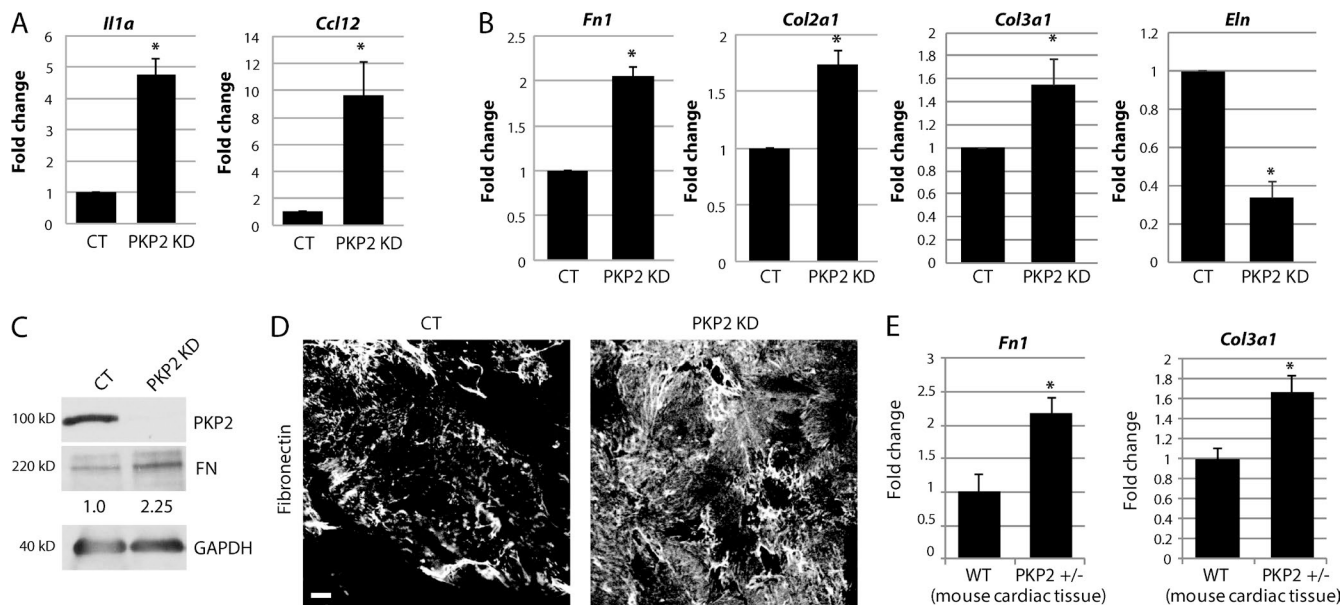
Figure 5. **Loss of PKP2 induces inflammatory and fibrotic gene expression.** (A and B) Freshly isolated neonatal CMs were infected with adenovirus containing either control (CT) or PKP2 KD constructs, and samples were analyzed 72 h postinfection. RNA isolated from control and PKP2 KD CMs were analyzed for mRNA levels of different genes by qPCR. KD of PKP2 in neonatal CMs resulted in a significant increase in mRNA levels of proinflammatory markers interleukin-1α (*Il1a*) and *Ccl12* (A) and ECM genes fibronectin (*Fn1*) and collagen (*Col2A1* and *Col3a1*) (B). Expression of Elastin (*Eln*) was reduced on loss of PKP2. (C) KD of PKP2 results in an increase in FN protein levels, as indicated by quantification of FN band intensity (normalized to GAPDH). (D) Control and PKP2 KD CMs were stained with an anti-FN antibody. KD of PKP2 results in an increase in FN expression as indicated by the increase in staining intensity of FN by immunofluorescence. Bar, 20 μm. (E) Analysis of RNA from wild-type (WT) and PKP2^{+/−} mouse hearts demonstrated a significant increase in expression of fibrotic genes such as *Fn1* and *Col3a1* on loss of PKP2 expression in vivo. All images and blots shown are representative of three independent experiments. For all graphs, fold change values from three or more independent samples are represented with error bars indicating SD. *, $P < 0.05$.

effects in different tissues (Brown et al., 2005; Moore et al., 2006; Souders et al., 2009; Aden et al., 2010; Falkenham et al., 2013; Fig. 5 A).

Loss of PKP2 also elevated expression of the ECM components fibronectin (*Fn1*) and collagen (*Col2a1* and *Col3a1*; Fig. 5 B). In contrast with fibronectin (FN) and collagen, expression of elastin (*Eln*) was decreased in response to PKP2 KD. This is particularly intriguing because increased matrix stiffness has been shown to exacerbate the effects of fibrosis in the heart and lungs (Engebretsen et al., 2014; Van Doren, 2015). Increased expression of FN in PKP2 KD cells was also observed by Western blot (Fig. 5 C) and by immunofluorescence (Fig. 5 D). Analysis of mouse heart samples indicated that haploinsufficiency of PKP2 also results in increased FN and collagen expression in vivo (Fig. 5 E). Increased expression of FN by CMs may indicate these cells are undergoing a transition to a mesenchymal phenotype on loss of PKP2. To analyze this, we investigated whether PKP2 KD caused an increase in expression of the mesenchymal markers Snail (*Snai1*), Snail-2/Slug (*Snai2*), and Vimentin (*Vim*), well known to be up-regulated on conversion of cells to a mesenchymal phenotype (Muraoka et al., 2014). However, *Snai1*, *Snai2*, and *Vim* mRNA were all unchanged compared with control CMs, suggesting that a mesenchymal transition is not occurring in these cells on loss of PKP2 (Fig. S3).

Abrogation of TGF-β1/p38 MAPK signaling in PKP2 KD CMs rescues fibrotic gene expression, but not adipogenesis

We next wanted to confirm that increased fibrotic gene expression seen in PKP2 KD CMs was indeed a result of elevated TGF-β1/p38 MAPK signaling. We therefore analyzed

the ability of inhibitors of the TGF-β1–p38 MAPK cascade to rescue the observed changes in expression of inflammatory/fibrotic genes. As expected, treatment of PKP2 KD CMs with (5Z)-7-Oxozeaenol curtailed the increase in *Ccl12* mRNA (Fig. 6 A) and *Fn1* mRNA (Fig. 6 B) seen on loss of PKP2. Oxozeaenol also rescued the increase in activation of STAT3 and NF-κB, suggesting that activation of these proinflammatory transcription factors in CMs is regulated by this MAPK cascade (Fig. 6, C and D). A previous study demonstrated an important role for PKP2 in the control of an adipogenic transcriptional program in CMs (Chen et al., 2014). As previously reported, we observed an increase in the adipogenic markers Adiponectin (*Adipoq*) and CEBPα (*Cebpa*) in CM cultures on loss of PKP2 (Fig. 6 E). Because increased fibrotic and adipogenic gene expression occurs concurrently in CMs on loss of PKP2, we sought to investigate whether there was cross talk between these transcriptional programs. Intriguingly, although inhibition of TGF-β1/p38 MAPK signaling by treatment with small molecule inhibitors was able to rescue inflammatory and fibrotic gene expression markers (Fig. 6, A and B), it did not curtail the increase in adipogenic genes upon PKP2 KD (Fig. 6 E). These data therefore indicate that fibrotic and adipogenic transcriptional programs occur via independent signaling mechanisms in CMs.

Loss of DP expression also promotes activation of TGF-β1/p38 MAPK signaling in cardiac cells

Although loss of PKP2 has been shown to dramatically affect DP localization in epithelial cells, changes in DP expression have not been observed in these cell types. We confirmed these previous findings by knocking down PKP2 in normal human
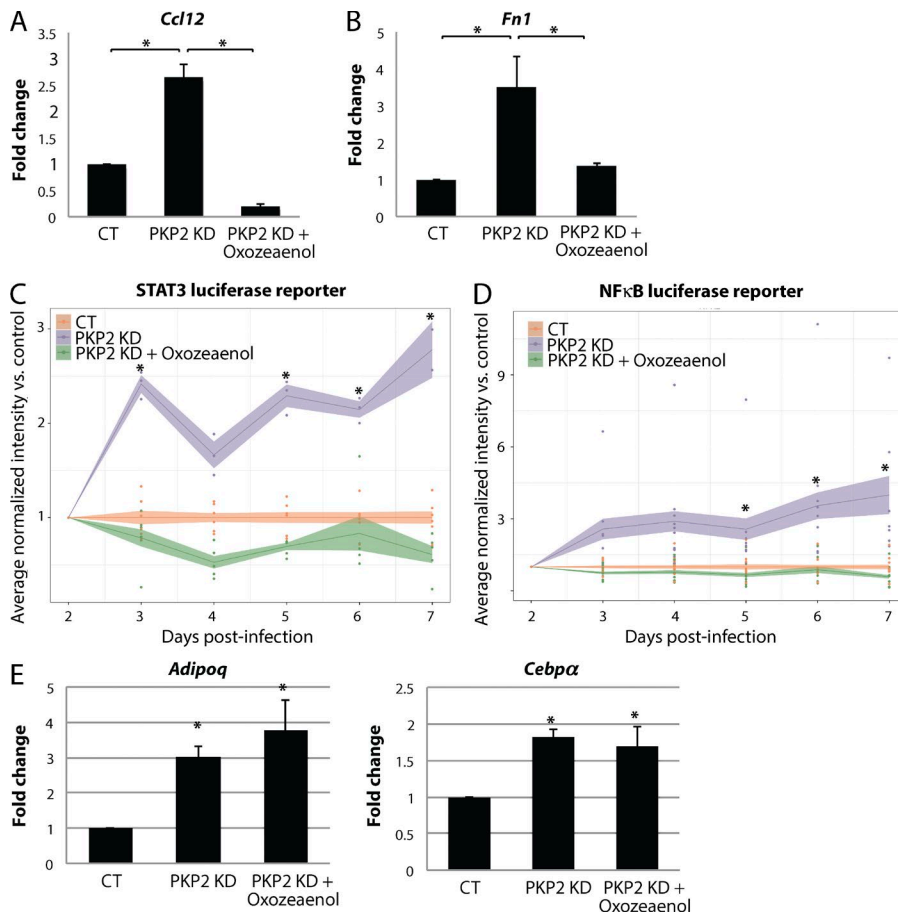
Figure 6. **Abrogation of TGF-β1/p38 MAPK signaling in PKP2 KD CMs rescues fibrotic gene expression, but not adipogenesis.** (A and B) Control (CT), PKP2 KD, and PKP2 KD CMs treated with the TAK1 inhibitor (5Z)-7-Oxozeaenol were analyzed for mRNA levels of *Ccl12* and fibronectin (*Fn1*). Treatment with oxozeaenol was able to rescue the increase in *Ccl12* and *Fn1* mRNA seen on loss of PKP2. (C and D) Control, PKP2 KD, and PKP2 KD CMs treated with oxozeaenol were analyzed for STAT3 and NF-κB transcriptional activity via luciferase reporter arrays. Luciferase expression followed in the same cells by noninvasive imaging for a period of 6 d indicated that TAK1 inhibition was able to rescue the increases in STAT3 and NF-κB transcriptional activity seen on KD of PKP2 in CMs. *, P < 0.05 for PKP2 KD values compared with PKP2 KD + oxozeaenol values. (E) RNA isolated from control and PKP2 KD CMs were analyzed for mRNA levels of adipogenic markers such as adiponectin (*Adipoq*) and CEBPα (*Cebpa*). *Adipoq* and *Cebpa* mRNA was increased on loss of PKP2 but could not be rescued by treatment with the TAK1 inhibitor oxozeaenol. For all graphs, fold change values from three or more independent samples are represented with error bars indicating SD. *, P < 0.05.

epidermal keratinocytes (NHEKs), which did not show any changes in either DP mRNA or protein levels compared with control cells (Fig. S4). In addition, PKP2 KD in NHEKs did not cause an increase in either TGF-β1 mRNA or p38 MAPK phosphorylation, consistent with the hypothesis that loss of DP expression is a causative factor in activation of this signaling pathway (Fig. S4).

To determine whether loss of DP expression in CMs upon PKP2 KD is a consequence of elevated TGF-β1/p38 MAPK signaling, we analyzed DP expression levels in PKP2 KD CMs treated with the TAK1 [(5Z)-7-Oxozeaenol] or p38 MAPK (SB203580) inhibitors. Treatment with either inhibitor was unable to rescue the loss of DP expression upon PKP2 KD (Fig. 7 A). In addition, neither the increase in DP solubility (Fig. 7 B) nor the loss of junctional localization of DP (Fig. 7 C) could be restored by inhibition of TGF-β1/p38 MAPK signaling. These data therefore indicate that loss of DP expression is not a result of increased TGF-β1/p38 MAPK signaling in these cells. To determine if DP expression is a causative event in promotion of TGF-β1/p38 MAPK signaling, we analyzed these markers in DP KD CMs. Interestingly, DP knockdown in CMs alone was sufficient to induce both increased *Tgfb1* mRNA levels and activation of p38 MAPK (Fig. 7 D). In addition, *Tgfb1* mRNA and p38 MAPK phosphorylation were increased in tissue samples from a mouse model harboring a conditional knockdown of DP in the epidermis, highlighting the importance of DP to activation of this signaling pathway in vivo (Vasioukhin et al., 2001; Fig. 7 E). Altogether, these data demonstrate that loss of DP expression occurs upstream of activation of TGF-β1/p38 MAPK signaling in PKP2 KD cells.

Rescue of DP expression in PKP2 KD cells restores normal levels of TGF-β1/p38 MAPK signaling

Finally, we tested the hypothesis that DP expression is a determining factor in up-regulation of TGF-β1/p38 MAPK signaling in PKP2 KD cells. To do this, we restored DP expression in a PKP2 KD background using DPII adenovirus. Lacking part of the DP rod domain, DPII is a naturally occurring shorter isoform of DPI (6.8 vs. 8.6 kb), and was used to overcome technical difficulties in size limits for adenoviral packaging and transduction. Just like DPI in wild-type cells, DPII localizes to DSMs and confers adhesive strength to junctions (Angst et al., 1990; Green et al., 1990; Cabral et al., 2012; Patel et al., 2014). Restoration of DP expression in a PKP2 KD background was indeed sufficient to rescue both the PKP2 KD–induced increased expression of *Tgfb1* mRNA (Fig. 8 A) and downstream phosphorylation of MKK3/6 and p38 MAPK (Fig. 8 B). In addition, restoration of DP expression rescued other phenotypes induced by loss of PKP2, such as increased levels of *Ccl12* mRNA and activation of the STAT3 transcription factor (Fig. 8, C and D). These data therefore identify the loss of DP as a crucial factor in triggering the up-regulation of TGF-β1/p38 MAPK signaling induced on loss of PKP2. Interestingly, unlike inhibition of TAK1 signaling, restoration of DP expression was also able to rescue the PKP2-induced increase in the adipogenic marker *Adipoq*. These data indicate that loss of DP expression is a proximal effect of PKP2 KD, which can trigger both fibrotic and adipogenic signaling pathways (Fig. 8 E). In summary, this study has identified a novel role for the DSM protein PKP2 in regulation of profibrotic gene expression in CMs, via a mechanism that includes regulation of DP expression and the TGF-β1/p38 MAPK signaling nexus.
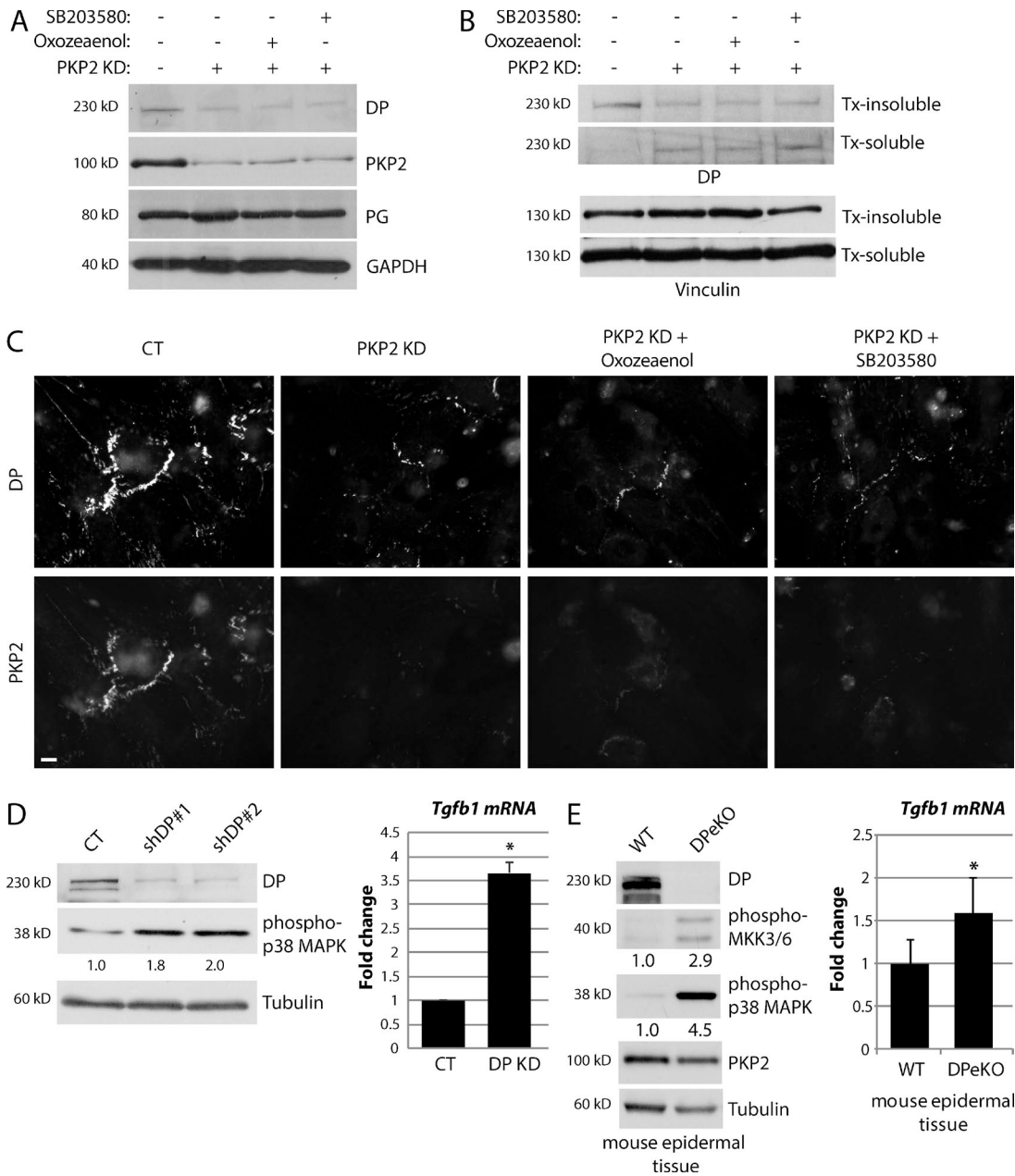
Figure 7. **Activation of TGF-β1/p38 MAPK signaling in cardiac cells is regulated by DP expression.** (A–C). Control (CT), PKP2 KD, and PKP2 KD CMs treated with either the TAK1 inhibitor (5Z)-7-oxozeaenol or p38 MAPK inhibitor SB203580 were analyzed for total protein levels of DP (A), solubility of DP using Triton X-100 fractionation assays (B), and junctional localization of DP (C). Neither TAK1 nor p38 MAPK inhibition was able to rescue the loss of DP protein expression, increase in DP solubility, or loss of junctional localization of DP, all of which are seen on loss of PKP2 KD in CMs. Bar, 20 µm. (D) Control and DP KD cells were analyzed for levels of phospho–p38 MAPK and *Tgfb1* mRNA, both of which were up-regulated on loss of DP expression. (E) Tissue samples from wild-type (WT) and DP epidermal knockout (DPeKO) mice were processed for protein and RNA analysis. Loss of DP expression resulted in activation of phospho–p38 MAPK and an increase in *Tgfb1* mRNA in the epidermis. For all graphs, fold change values from three or more independent samples are represented with error bars indicating SD. *, P < 0.05.

Discussion

Although the DSM has a well-known function in maintaining cell–cell mechanical stability, DSM proteins have also recently emerged as modulators of intracellular signaling. We and others have shown that the DSM armadillo proteins PKP2 and PG modulate Rho GTPases, epidermal growth factor receptor, and other signaling pathways (Godsel et al., 2010; Todorović et al., 2010; Arimoto et al., 2014). Here we have identified a role for PKP2 in controlling the activity of the TGF-β1/p38 MAPK signaling

nexus in cardiac cells. On loss of PKP2 either in vitro or in vivo, TGF-β1 levels are increased, which leads to an activation of the TAK1–MKK3/6–p38 MAPK signaling cascade. Increased TGF-β1/p38 MAPK signaling results in elevated expression of profibrotic cytokines and ECM proteins, such as FN and collagen. Activation of this signaling pathway can be rescued by restoration of DP expression, which is lost upon PKP2 KD.

Our previous studies in epithelial cells have demonstrated an important role for PKP2 in regulation of DP localization (Bass-Zubek et al., 2008). We have also shown that PKP2
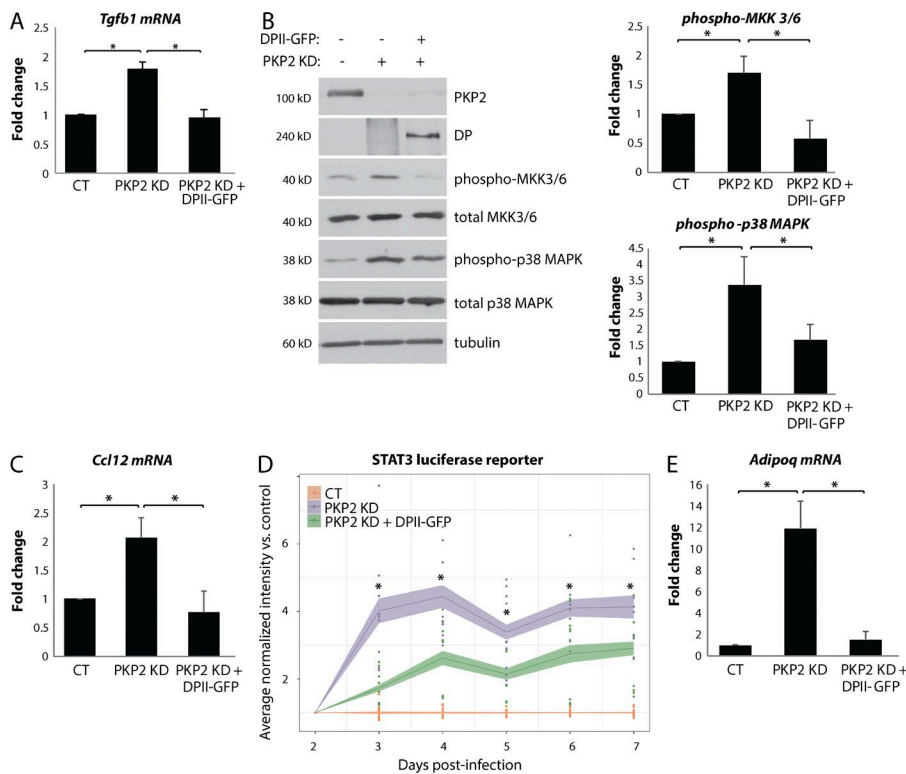
Figure 8. Rescue of DP expression in PKP2 KD cells restores normal levels of TGF-β1/p38 MAPK signaling. (A–E) Freshly isolated neonatal CMs were infected with adenovirus containing control, PKP2 KD, or PKP2 KD + DPII-GFP constructs. 72 h postinfection, cells were analyzed for mRNA levels of *Tgfb1* (A), *Ccl12* (C), or *Adipoq* (E) by qPCR, blotted for phosphorylated forms of MKK3/6 and p38 MAPK (quantified in the graphs, right panels) (B), or analyzed for STAT3 transcriptional activity via luciferase reporter arrays (D). *, P < 0.05 for PKP2 KD values compared with PKP2 KD + DPII-GFP values. The induction of all of these phenotypes observed on loss of PKP2 were rescued by re-expression of DPII-GFP. All images and blots shown are representative of three independent experiments. For all graphs, fold change values from three or more independent samples are represented with error bars indicating SD. *, P < 0.05.

regulates RhoA GTPase signaling and actin cytoskeletal rearrangements to promote localization of DP to cell–cell junctions (Godsel et al., 2010). Although loss of PKP2 in epithelial cells results in mislocalization of DP, its expression levels are unchanged. In contrast, we show here that PKP2 KD in cardiac cells results in defective DP localization and decreased stability and degradation by the proteasome (Fig. 1). The differences in DP stability upon loss of PKP2 may reflect inherent differences in the composition and organization of the cell–cell junctions in these different cell types. Although epithelial cells have separate AJs and DSMs, CMs display hybrid junctions called *area composita*, containing components of both AJs and DSMs (Franke et al., 2006, 2007). Loss of PKP2 in neonatal CMs resulted in a major defect in cell–cell adhesion in these cells (Sato et al., 2011). Tethering of DP in cardiac junctions is dependent on PKP2 because it is the only PKP expressed in CMs, unlike epithelial cells that also express PKP1 (differentiated epithelia) and PKP3 (simple/stratified epithelia; Bass-Zubek et al., 2009).

Multiple studies have characterized the importance of catenin proteins expressed in cardiac tissue (such as PG and αT-catenin) in development of arrhythmogenic phenotypes in AC (Li et al., 2011; Swope et al., 2012, 2013). Mutations in PKP2 are frequently identified in cases of AC, a disease that displays a triad of phenotypes, including arrhythmia, loss of healthy myocardial cells, and loss of fibro-fatty deposits (Fidler et al., 2009; Delmar and McKenna, 2010). Loss of PKP2 was shown to promote adipogenic gene transcription in CMs via activation of the Hippo pathway and suppression of β-catenin/YAP signaling (Chen et al., 2014). In this study, we asked whether loss of PKP2 might also trigger known profibrotic signaling pathways. Although deposition of ECM commonly occurs after heart injury, fibrosis represents a pathological misregulation of this normal reparative process (Klingberg et al., 2013). Fibrosis is a major factor in heart failure resulting from multiple conditions such as myocardial infarction, high blood pressure, and

diabetes (Awad et al., 2008; Edgley et al., 2012; Pearson et al., 2013). Fibrosis can result in an increase in stiffness, increased CM atrophy, and loss of electrical conductivity and arrhythmia (Jellis et al., 2010; Krenning et al., 2010; Weber et al., 2013).

TGF-β1 is well known as a potent profibrotic cytokine that induces robust ECM production (Leask and Abraham, 2004; Leask, 2007; Biernacka et al., 2011; Dobaczewski et al., 2011). Global gene expression studies have indicated that profibrotic inflammatory mediators are up-regulated in p38 MAPK–activated hearts (Clerk and Sugden, 2006; Tenhunen et al., 2006). Myocardial infarction in rats has been shown to cause TGF-β–dependent activation of p38 MAPK via the upstream kinases TAK1 and MKK3/6 (Zhang et al., 2000; Derynck and Zhang, 2003; Matsumoto-Ida et al., 2006). The TAK1–MKK3–p38 MAPK cascade is also important for TGF-β–induced ECM production (Ono et al., 2003; Kim et al., 2007). Indeed, increases in FN gene expression seen upon PKP2 KD were rescued by the TAK1 inhibitor (5Z)-7-Oxozeaenol. These data are recapitulated in cardiac tissue from a PKP2 heterozygous mouse model, which showed that TGF-β1 mRNA, p38 MAPK activation, and fibrotic gene expression are all elevated in PKP2^{+/−} cells compared with controls. This evidence suggests that this profibrotic signaling pathway can be stimulated by haploinsufficiency of PKP2, which mimics known mutations of PKP2 found in cases of AC, resulting in partial loss of PKP2 expression (Kirchner et al., 2012). A recent study implicated p38 MAPK in PG-dependent regulation of keratinocyte cohesion, suggesting that other DSM proteins might also regulate p38 MAPK signaling (Gordon et al., 2011; Hartlieb et al., 2014; Spindler et al., 2014).

Downstream of TGF-β, p38 MAPK can influence a variety of proinflammatory transcription factors, such as STAT3 and NF-κB, which we demonstrate are activated in response to loss of PKP2 in CMs (Craig et al., 2000; Haghikia et al., 2011, 2014). Interestingly, a recent study demonstrated an increase in myocardial staining and serum levels of inflammatory

markers in patients with AC, highlighting the importance of p38 MAPK–mediated inflammatory signaling in AC pathogenesis (Asimaki et al., 2011). Activation of p38 MAPK has been observed in both animal models of heart failure and myocardial biopsies from patients with heart failure (Takeishi et al., 2002; Bellahcene et al., 2006). Our findings add support to the idea that pharmacologic inhibitors of p38 MAPK should be explored further as treatment for patients with heart failure.

Importantly, we demonstrate that loss of PKP2 in CMs resulted in increased expression of multiple secreted factors (TGF-β1, interleukin-1α, and CCL12), all of which are known to promote profibrotic gene expression in both CMs and CFs (Manabe et al., 2002). Although the precise signaling mechanism has not been well established, multiple studies have demonstrated the ability of different interleukins, such as interleukin-1α, to induce cell migration or ECM expression in CFs (Brown et al., 2005; Wynn, 2008; Souders et al., 2009; Aden et al., 2010; Wynn and Ramalingam, 2012). CCL12 has been shown to play a role in pulmonary fibrosis (Moore et al., 2006) and also induces proliferation of fibrocytes, which are fibroblast progenitor cells involved in cardiac fibrosis (Falkenham et al., 2013). We therefore hypothesize that in addition to autocrine activation of fibrotic gene expression in CMs, increased expression of these profibrotic secreted factors on loss of PKP2 would promote paracrine activation of fibrotic gene expression in CFs as well. These data are supported by our finding that activation of p38 MAPK in CMs is non–cell autonomous (Fig. S2 B).

Activation of TGF-β1/p38 MAPK signaling on loss of PKP2 seems to be specific to CMs, because we did not observe such activation in epithelial cells. It is plausible to suggest that other PKPs may compensate for the loss of PKP2 in epithelial cells, because PKPs have been shown to have some redundant functions (Hatzfeld, 2007; Bass-Zubek et al., 2009). However, our initial findings with combinatorial knockdown of PKP1, 2, and 3 in epithelial cells did not produce a significant increase in phospho–p38 MAPK levels. These data suggest that redundancy of PKPs alone may not be sufficient to explain this lack of phenotype in epithelial cells. Because loss of DP upon PKP2 KD occurs only in CMs, we investigated whether triggering TGF-β1/p38 MAPK signaling was dependent on expression of DP. Indeed, DP KD alone in CMs induced TGF-β1/p38 MAPK signaling. Conditional loss of DP in mouse epidermal tissue recapitulated these results in vivo, supporting the hypothesis that loss of DP expression upon PKP2 KD is the determining factor in induction of TGF-β1/p38 MAPK signaling. Further, restoration of DP expression rescued the multiple profibrotic phenotypes observed on loss of PKP2, such as elevated *Tgfb1 and Ccl12* mRNA levels and activation of p38 MAPK and STAT3. Importantly, unlike TAK1 inhibition, DP restoration also rescued the PKP2 KD–dependent increase in the adipogenic marker *Adipoq*. Collectively, these data indicate specificity of TGF-β1/p38 MAPK signaling to profibrotic responses induced by PKP2 loss and implicate DP as a key intermediary in the regulation of both profibrotic and adipogenic gene expression by PKP2. These studies have identified TGF-β1/p38 MAPK signaling as a mechanistic link between loss of the DSM armadillo protein PKP2 and aberrant regulation of fibrotic gene expression. Identification of profibrotic triggers such as TGF-β1/p38 MAPK signaling downstream of PKP2 KD has relevance for the study of AC and also other cardiac diseases in which junctional remodeling and fibrosis are major components, such as hypertrophic and dilated cardiomyopathies.

Materials and methods

Isolation of neonatal CMs, cell cultures, and mouse models

Cultures of neonatal rat ventricular CMs were prepared as previously described (Sato et al., 2009) from 1- to 3-d-old Sprague-Dawley rats (Charles River). Extracted neonatal hearts were finely minced, enzymatically digested, and resuspended in M199 medium containing 10% FBS and 15 µM of vitamin B12. After a 2-h preplating step to separate out quickly adhering cardiac fibroblasts (CFs), the cell suspension was filtered through a 40-µm filter, spun, and resuspended in M199 medium containing 10% horse serum, 15 µM vitamin B12, and BrdU. Resuspended cells were then plated in six-well dishes or coverslips precoated with collagen type IV, and medium was changed every 24–48 h. Adenoviral infection was performed 48 h after isolation. These protocols were conducted with the approval of the Northwestern University Institutional Animal Care and Use Committee, and all animal care protocols conform to National Institutes of Health guidelines and the recommendations of the Panel on Euthanasia of the American Veterinary Medical Association. The HL-1 cell line was maintained in Claycomb Medium (Sigma-Aldrich) supplemented with 10% FBS (Atlanta Biologicals), 0.1 mM norepinephrine, 2 mM L-glutamine, and penicillin/streptomycin solution (Sigma-Aldrich) and cultured on dishes precoated with a solution of FN-0.02% gelatin. NHEKs were obtained from the Northwestern University Skin Disease Research Center. These cells were grown in medium 154 containing human keratinocyte growth supplement, gentamycin/amphotericin B solution (Invitrogen), and 0.07 mM CaCl$_2$. Frozen samples of wild-type and PKP2$^{+/-}$ mouse hearts (Cerrone et al., 2012) were obtained from M. Delmar (New York University School of Medicine, New York, NY). Mouse hearts were snap frozen in liquid nitrogen and homogenized in either urea sample buffer (8 M deionized urea, 1% SDS, 10% glycerol, 60 mM Tris, pH 6.8, and 5% β-mercaptoethanol) for protein analysis or in Buffer RLT (RNeasy Mini kit; Qiagen) for qPCR analysis. Conditional gene targeting was used to specifically ablate the DP gene in developing mouse epidermis. Exon 2 of the DP gene is flanked with LoxP sites (Vasioukhin et al., 2001) and removed by breeding with mice transgenic for Cre recombinase under the control of the keratin 14 promoter (Vasioukhin et al., 1999). Both the DP-floxed and the K14-Cre transgenic mice were gifts from E. Fuchs (Rockefeller University, New York, NY). Skins from E18.5 embryos were snap frozen in liquid nitrogen and processed for either Western blotting or RNA analysis as described earlier in this paragraph.

DNA and KD constructs, adenovirus production, and chemical reagents

Human C-terminally V5-tagged PKP2 was generated by cloning PKP2 into the pCDNA 3.2/V5 DEST vector using Gateway technology (Invitrogen). GFP-tagged DPII was generated using the QuikChange II XL Site-Directed Mutagenesis kit (Agilent Technologies) to splice out nucleotides 3,584–5,380 of a GFP-tagged construct of full-length human DPI (Godsel et al., 2005). Adenoviral DPII constructs were generated by cloning DPII-GFP into the pAd CMV/V5-DEST vector using Gateway recombination. For KD constructs, the EmGFP BLOCK-iT PolII miR RNAi Expression Vector kit (Life Technologies) was used to design and clone control, rat PKP2-specific oligonucleotides (target sequences: 5′-TGTGAATATGCT-GGATGCAGA-3′ and 5′-TGGAACTTGTCCTCTAGTGAT-3′) and rat DP-specific oligonucleotides (target sequences: 5′-AAACCGGAAACAT-CATCTCTT-3′ and 5′-TGGTAATAGTTGACCCAGAAA-3′). These constructs were cloned into the pAd CMV/V5-DEST vector using Gateway recombination and used to generate virus using the ViraPower Adenoviral Expression System (Invitrogen). Where indicated, CMs were treated with the following compounds obtained from EMD Millipore: 10 µg/ml cycloheximide, 0.5 µM (5Z)-7-Oxozeaenol, 1 µM SB203580, 10 µM SB431542, 100 µM chloroquine, 10 µM MG132, and 2 ng/ml TGF-β1 ligand.

qPCR

For measurement of mRNA transcript levels using qPCR, RNA was isolated using the RNeasy Mini kit, according to manufacturer's instructions. Total RNA concentrations were equalized between samples, and cDNA was prepared using the Superscript III First Strand kit (Invitrogen). qPCR was performed using SYBR Green PCR master mix (Applied Biosystems) and gene-specific primers in a StepOnePlus instrument (Applied Biosystems). Calculations for relative mRNA levels were performed using the $\Delta\Delta Ct$ method, normalized to GAPDH, and represented as fold-change values compared with control samples. Statistical analysis was performed using a two-tailed t test. P values <0.05 were considered statistically significant.

Western blotting and biochemical assays

To analyze protein expression levels, cells were washed briefly in PBS and lysed in urea sample buffer (8 M deionized urea, 1% SDS, 10% glycerol, 60 mM Tris, pH 6.8, and 5% β-mercaptoethanol) and equalized for total protein concentration. For Triton solubility assays, cells were lysed in a buffer containing 150 mM NaCl, 50 mM Tris, pH 7.6, 1% Triton X-100, and protease inhibitors. Lysates were incubated for 5 min on ice with gentle pipetting, and Triton X-100–soluble and –insoluble fractions were separated by centrifugation. All samples were subjected to SDS-PAGE on 7.5% or 10% polyacrylamide gels, followed by transfer to polyvinylidene fluoride membranes (Millipore). Membranes were probed with specific primary and secondary antibodies (see Antibodies section) and visualized using enhanced chemiluminescence and x-ray film (Thermo Fisher Scientific). All Western blots shown are representative data obtained from three independent experiments. For densitometric analysis of Western blots, films were scanned using Officejet 5610 scan software (Hewlett-Packard) and analyzed using ImageJ software (National Institutes of Health). Error bars for densitometric analysis represent SD. Measurement of TGF-β1 levels in cell culture supernatants was performed using the TGF-β1 immunoassay (R&D Systems) according to the manufacturer's protocol. Statistical analysis was performed using a two-tailed t test. P-values <0.05 were considered statistically significant.

Immunofluorescence and quantification of fluorescence pixel intensity

For immunofluorescence, cells grown on coverslips were fixed in 4% paraformaldehyde or ice-cold methanol and permeabilized with 0.2% Triton X-100 in PBS. Primary and secondary antibody incubations were performed at RT for 1 h, interspaced by multiple washes in PBS, and followed by mounting coverslips in polyvinyl alcohol (Sigma-Aldrich). Fixed cells were visualized with a Leica microscope (model DMR) fitted with 40- (NA 1.0, Plan-Fluotar) and 63-Å (NA 1.32, Plan-Apochromat) objective lenses and images captured with an Orca 100 CCD camera (model C4742-95; Hamamatsu) and Metamorph 7.7 imaging software (Molecular Devices). Confocal imaging was performed at the Northwestern University Cell Imaging Facility using a LSM 510 META confocal microscope (Carl Zeiss) fitted with 63- or 100-Å objective lenses (NAs 1.32 and 1.4, Plan Apochromat; Carl Zeiss) and LSM 510 software. Quantification of mean fluorescence pixel intensity was performed from raw, unsaturated 12-bit images by tracing cell–cell junctions using ImageJ. For all quantification analyses, control and treatment/knockdown conditions were imaged on the same day using the same instruments and exposure settings, and quantification was performed on 10–20 randomly imaged areas per experimental group. Error bars for fluorescence pixel-intensity measurements represent SEMs. Statistical analysis was performed using a two-tailed t test. P values <0.05 were considered statistically significant.

Antibodies

The following primary antibodies were used: mouse anti-PKP2 (651101; Progen), 1407 chicken anti-Pg (Aves Laboratories), NW161 rabbit anti-DP directed against the first 189 amino acids of DP (Bornslaeger et al., 1996), mouse anti-PKP2, mouse anti–β-catenin, mouse anti–p120-catenin (BD), rabbit anti-Cx43 (AB1728; EMD Millipore), mouse anti–N-cadherin, mouse anti-V5 (Invitrogen), mouse anti-desmin, rabbit anti-GAPDH, rabbit anti-FN, rabbit anti-GFP (Sigma-Aldrich), 12G10 mouse anti-tubulin (Developmental Studies Hybridoma Bank), rabbit anti–phospho-TAK1, rabbit anti–phospho-MKK3/6, rabbit anti-MKK3, rabbit anti–phospho-p38 MAPK, and rabbit anti–p38 MAPK (Cell Signaling Technologies). For experiments including re-expression of human V5-tagged PKP2 in rat PKP2 KD CMs, a pool of two antibodies (Progen and BD) was used to analyze PKP2 levels because anti-PKP2 from Progen alone does not recognize exogenously expressed human V5-tagged PKP2 (likely because of the epitope at the C-terminal end being masked by the V5 tag) and anti-human PKP2 from BD alone does not recognize endogenous rat PKP2. Secondary antibodies for Western blotting included HRP-conjugated goat anti–mouse, –rabbit, and –chicken antibodies (Kirkegaard and Perry Laboratories). Secondary antibodies for immunofluorescence included Alexa Fluor 488–, 568–, or 647–conjugated goat anti–mouse, –rabbit, and –chicken antibodies (Invitrogen).

Transcription factor arrays

Transcription factor arrays were performed as previously described (Bellis et al., 2013; Siletz et al., 2013; Aguado et al., 2015). CMs were plated in black, clear-bottom, 96-well plates and infected with lentiviral vectors containing transcription factor binding reporter constructs driving the expression of firefly luciferase. Cells plated without virus infection served as negative controls to determine signal background levels. TATA–firefly luciferase reporter constructs without any additional transcription factor binding elements were used as positive controls to determine basal promoter activity. Each transcription factor reporter is represented with $n = 4$ measurements for each condition tested, and each plate was repeated a total of three times. To measure transcription factor activity, ᴅ-luciferin (RR Labs) diluted in the appropriate media was added to wells in excess to a final concentration of 2 mM. After a 45-min incubation period with ᴅ-luciferin, luminescence was quantified using an IVIS Lumina LTE imaging system (Caliper Life Sciences). Luminescence readings measured as photon flux (photons/second) from each well were collected every day for 6 d. Media was exchanged every other day. To normalize values and determine statistical significance, array data were log2 transformed and filtered to eliminate all intensities below background (P < 0.05). The background was defined as the mean measured intensity in noninfected cells subject to the same treatment at the same time and plate. The TATA box promoter control reporter and the control condition were used to normalize reporter activity at each time point. Normalized values that were identified to be outliers (P < 0.003) for each reporter were removed. Normalized log2 transcription factor activity of each condition was compared directly with control conditions using the limma package in R. False discovery rate was used to correct for multiple comparisons. Transcription factors identified to be differentially active had an adjusted p-value of <0.05.

Online supplemental material

Fig. S1 demonstrates that loss of PKP2 in CMs does not induce the activation of the transcription factors AP1 and MEF2. Fig. S2 shows that PKP2 KD activates p38 MAPK in desmin-positive CMs and that this activation can occur in a non–cell-autonomous fashion. Fig. S3 confirms that PKP2 loss does not induce the expression of

mesenchymal markers in CMs. Fig. S4 shows that KD of PKP2 in NHEKs does not produce the same phenotypes as seen in CMs (e.g., loss of DP expression or an increase in TGF-β1/p38 MAPK signaling). Online supplemental material is available at http://www.jcb.org/cgi/content/full/jcb.201507018/DC1.

References

Aden, N., A. Nuttall, X. Shiwen, P. de Winter, A. Leask, C.M. Black, C.P. Denton, D.J. Abraham, and R.J. Stratton. 2010. Epithelial cells promote fibroblast activation via IL-1alpha in systemic sclerosis. *J. Invest. Dermatol.* 130:2191–2200. http://dx.doi.org/10.1038/jid.2010.120

Aguado, B.A., J.J. Wu, S.M. Azarin, D. Nanavati, S.S. Rao, G.G. Bushnell, C.B. Medicherla, and L.D. Shea. 2015. Secretome identification of immune cell factors mediating metastatic cell homing. *Sci. Rep.* 5:17566. http://dx.doi.org/10.1038/srep17566

Angst, B.D., L.A. Nilles, and K.J. Green. 1990. Desmoplakin II expression is not restricted to stratified epithelia. *J. Cell Sci.* 97:247–257.

Arimoto, K., C. Burkart, M. Yan, D. Ran, S. Weng, and D.-E.E. Zhang. 2014. Plakophilin-2 promotes tumor development by enhancing ligand-dependent and -independent epidermal growth factor receptor dimerization and activation. *Mol. Cell. Biol.* 34:3843–3854. http://dx.doi.org/10.1128/MCB.00758-14

Asimaki, A., H. Tandri, E.R. Duffy, J.R. Winterfield, S. Mackey-Bojack, M.M. Picken, L.T. Cooper, D.J. Wilber, F.I. Marcus, C. Basso, et al. 2011. Altered desmosomal proteins in granulomatous myocarditis and potential pathogenic links to arrhythmogenic right ventricular cardiomyopathy. *Circ Arrhythm Electrophysiol.* 4:743–752. http://dx.doi.org/10.1161/CIRCEP.111.964890

Awad, M.M., H. Calkins, and D.P. Judge. 2008. Mechanisms of disease: molecular genetics of arrhythmogenic right ventricular dysplasia/cardiomyopathy. *Nat. Clin. Pract. Cardiovasc. Med.* 5:258–267. http://dx.doi.org/10.1038/ncpcardio1182

Bass-Zubek, A.E., R.P. Hobbs, E.V. Amargo, N.J. Garcia, S.N. Hsieh, X. Chen, J.K. Wahl III, M.F. Denning, and K.J. Green. 2008. Plakophilin 2: a critical scaffold for PKC alpha that regulates intercellular junction assembly. *J. Cell Biol.* 181:605–613. http://dx.doi.org/10.1083/jcb.200712133

Bass-Zubek, A.E., L.M. Godsel, M. Delmar, and K.J. Green. 2009. Plakophilins: multifunctional scaffolds for adhesion and signaling. *Curr. Opin. Cell Biol.* 21:708–716. http://dx.doi.org/10.1016/j.ceb.2009.07.002

Bellahcene, M., S. Jacquet, X.B. Cao, M. Tanno, R.S. Haworth, J. Layland, A.M. Kabir, M. Gaestel, R.J. Davis, R.A. Flavell, et al. 2006. Activation of p38 mitogen-activated protein kinase contributes to the early cardiodepressant action of tumor necrosis factor. *J. Am. Coll. Cardiol.* 48:545–555. http://dx.doi.org/10.1016/j.jacc.2006.02.072

Bellis, A.D., B.P. Bernabé, M.S. Weiss, S. Shin, S. Weng, L.J. Broadbelt, and L.D. Shea. 2013. Dynamic transcription factor activity profiling in 2D and 3D cell cultures. *Biotechnol. Bioeng.* 110:563–572. http://dx.doi.org/10.1002/bit.24718

Biernacka, A., M. Dobaczewski, and N.G. Frangogiannis. 2011. TGF-β signaling in fibrosis. *Growth Factors.* 29:196–202. http://dx.doi.org/10.3109/08977194.2011.595714

Bornslaeger, E.A., C.M. Corcoran, T.S. Stappenbeck, and K.J. Green. 1996. Breaking the connection: displacement of the desmosomal plaque protein desmoplakin from cell-cell interfaces disrupts anchorage of intermediate filament bundles and alters intercellular junction assembly. *J. Cell Biol.* 134:985–1001. http://dx.doi.org/10.1083/jcb.134.4.985

Borrmann, C.M., C. Grund, C. Kuhn, I. Hofmann, S. Pieperhoff, and W.W. Franke. 2006. The area composita of adhering junctions connecting heart muscle cells of vertebrates. II. Colocalizations of desmosomal and fascia adhaerens molecules in the intercalated disk. *Eur. J. Cell Biol.* 85:469–485. http://dx.doi.org/10.1016/j.ejcb.2006.02.009

Brown, R.D., S.K. Ambler, M.D. Mitchell, and C.S. Long. 2005. The cardiac fibroblast: therapeutic target in myocardial remodeling and failure. *Annu. Rev. Pharmacol. Toxicol.* 45:657–687. http://dx.doi.org/10.1146/annurev.pharmtox.45.120403.095802

Cabral, R.M., D. Tattersall, V. Patel, G.D. McPhail, E. Hatzimasoura, D.J. Abrams, A.P. South, and D.P. Kelsell. 2012. The DSPII splice variant is crucial for desmosome-mediated adhesion in HaCaT keratinocytes. *J. Cell Sci.* 125:2853–2861. http://dx.doi.org/10.1242/jcs.084152

Cerrone, M., M. Noorman, X. Lin, H. Chkourko, F.-X.X. Liang, R. van der Nagel, T. Hund, W. Birchmeier, P. Mohler, T.A. van Veen, et al. 2012. Sodium current deficit and arrhythmogenesis in a murine model of plakophilin-2 haploinsufficiency. *Cardiovasc. Res.* 95:460–468. http://dx.doi.org/10.1093/cvr/cvs218

Chen, S.N., P. Gurha, R. Lombardi, A. Ruggiero, J.T. Willerson, and A.J. Marian. 2014. The hippo pathway is activated and is a causal mechanism for adipogenesis in arrhythmogenic cardiomyopathy. *Circ. Res.* 114:454–468. http://dx.doi.org/10.1161/CIRCRESAHA.114.302810

Clerk, A., and P.H. Sugden. 2006. Inflame my heart (by p38-MAPK). *Circ. Res.* 99:455–458. http://dx.doi.org/10.1161/01.RES.0000241053.89089.c3

Craig, R., A. Larkin, A.M. Mingo, D.J. Thuerauf, C. Andrews, P.M. McDonough, and C.C. Glembotski. 2000. p38 MAPK and NF-kappa B collaborate to induce interleukin-6 gene expression and release. Evidence for a cytoprotective autocrine signaling pathway in a cardiac myocyte model system. *J. Biol. Chem.* 275:23814–23824. http://dx.doi.org/10.1074/jbc.M909695199

Delmar, M., and W.J. McKenna. 2010. The cardiac desmosome and arrhythmogenic cardiomyopathies: from gene to disease. *Circ. Res.* 107:700–714. http://dx.doi.org/10.1161/CIRCRESAHA.110.223412

Derynck, R., and Y.E. Zhang. 2003. Smad-dependent and Smad-independent pathways in TGF-beta family signalling. *Nature.* 425:577–584. http://dx.doi.org/10.1038/nature02006

Dobaczewski, M., and N.G. Frangogiannis. 2009. Chemokines and cardiac fibrosis. *Front. Biosci. (Schol. Ed.).* 1:391–405. http://dx.doi.org/10.2741/s33

Dobaczewski, M., W. Chen, and N.G. Frangogiannis. 2011. Transforming growth factor (TGF)-β signaling in cardiac remodeling. *J. Mol. Cell. Cardiol.* 51:600–606. http://dx.doi.org/10.1016/j.yjmcc.2010.10.033

Edgley, A.J., H. Krum, and D.J. Kelly. 2012. Targeting fibrosis for the treatment of heart failure: a role for transforming growth factor-β. *Cardiovasc. Ther.* 30:e30–e40. http://dx.doi.org/10.1111/j.1755-5922.2010.00228.x

Engebretsen, K.V., K. Skårdal, S. Bjørnstad, H.S. Marstein, B. Skrbic, I. Sjaastad, G. Christensen, J.L. Bjørnstad, and T. Tønnessen. 2014. Attenuated development of cardiac fibrosis in left ventricular pressure overload by SM16, an orally active inhibitor of ALK5. *J. Mol. Cell. Cardiol.* 76:148–157. http://dx.doi.org/10.1016/j.yjmcc.2014.08.008

Falkenham, A., M. Sopel, N. Rosin, T.D. Lee, T. Issekutz, and J.-F.F. Légaré. 2013. Early fibroblast progenitor cell migration to the AngII-exposed myocardium is not CXCL12 or CCL2 dependent as previously thought. *Am. J. Pathol.* 183:459–469. http://dx.doi.org/10.1016/j.ajpath.2013.04.011

Fidler, L.M., G.J. Wilson, F. Liu, X. Cui, S.W. Scherer, G.P. Taylor, and R.M. Hamilton. 2009. Abnormal connexin43 in arrhythmogenic right ventricular cardiomyopathy caused by plakophilin-2 mutations. *J. Cell. Mol. Med.* 13:4219–4228. http://dx.doi.org/10.1111/j.1582-4934.2008.00438.x

Franke, W.W., C.M. Borrmann, C. Grund, and S. Pieperhoff. 2006. The area composita of adhering junctions connecting heart muscle cells of vertebrates. I. Molecular definition in intercalated disks of cardiomyocytes by immunoelectron microscopy of desmosomal proteins. *Eur. J. Cell Biol.* 85:69–82. http://dx.doi.org/10.1016/j.ejcb.2005.11.003

Franke, W.W., H. Schumacher, C.M. Borrmann, C. Grund, S. Winter-Simanowski, T. Schlechter, S. Pieperhoff, and I. Hofmann. 2007. The area composita of adhering junctions connecting heart muscle cells of vertebrates - III: assembly and disintegration of intercalated disks in rat cardiomyocytes growing in culture. *Eur. J. Cell Biol.* 86:127–142. http://dx.doi.org/10.1016/j.ejcb.2006.11.003

Gandjbakhch, E., P. Charron, V. Fressart, G. Lorin de la Grandmaison, F. Simon, F. Gary, A. Vite, B. Hainque, F. Hidden-Lucet, M. Komajda, and E. Villard. 2011. Plakophilin 2A is the dominant isoform in human heart tissue: consequences for the genetic screening of arrhythmogenic right ventricular cardiomyopathy. *Heart.* 97:844–849. http://dx.doi.org/10.1136/hrt.2010.205880

Garcia-Gras, E., R. Lombardi, M.J. Giocondo, J.T. Willerson, M.D. Schneider, D.S. Khoury, and A.J. Marian. 2006. Suppression of canonical Wnt/beta-catenin signaling by nuclear plakoglobin recapitulates phenotype of arrhythmogenic right ventricular cardiomyopathy. *J. Clin. Invest.* 116:2012–2021. http://dx.doi.org/10.1172/JCI27751

Godsel, L.M., S.N. Hsieh, E.V. Amargo, A.E. Bass, L.T. Pascoe-McGillicuddy, A.C. Huen, M.E. Thorne, C.A. Gaudry, J.K. Park, K. Myung, et al. 2005. Desmoplakin assembly dynamics in four dimensions: multiple phases differentially regulated by intermediate filaments and actin. *J. Cell Biol.* 171:1045–1059. http://dx.doi.org/10.1083/jcb.200510038

Godsel, L.M., A.D. Dubash, A.E. Bass-Zubek, E.V. Amargo, J.L. Klessner, R.P. Hobbs, X. Chen, and K.J. Green. 2010. Plakophilin 2 couples actomyosin remodeling to desmosomal plaque assembly via RhoA. *Mol. Biol. Cell.* 21:2844–2859. http://dx.doi.org/10.1091/mbc.E10-02-0131

Goossens, S., B. Janssens, S. Bonné, R. De Rycke, F. Braet, J. van Hengel, and F. van Roy. 2007. A unique and specific interaction between alphaT-catenin and plakophilin-2 in the area composita, the mixed-type junctional structure of cardiac intercalated discs. *J. Cell Sci.* 120:2126–2136. http://dx.doi.org/10.1242/jcs.004713

Gordon, J.W., J.A. Shaw, and L.A. Kirshenbaum. 2011. Multiple facets of NF-κB in the heart: to be or not to NF-κB. *Circ. Res.* 108:1122–1132. http://dx.doi.org/10.1161/CIRCRESAHA.110.226928

Green, K.J., and C.L. Simpson. 2007. Desmosomes: new perspectives on a classic. *J. Invest. Dermatol.* 127:2499–2515. http://dx.doi.org/10.1038/sj.jid.5701015

Green, K.J., D.A. Parry, P.M. Steinert, M.L. Virata, R.M. Wagner, B.D. Angst, and L.A. Nilles. 1990. Structure of the human desmoplakins. Implications for function in the desmosomal plaque. *J. Biol. Chem.* 265:11406–11407.

Grossmann, K.S., C. Grund, J. Huelsken, M. Behrend, B. Erdmann, W.W. Franke, and W. Birchmeier. 2004. Requirement of plakophilin 2 for heart morphogenesis and cardiac junction formation. *J. Cell Biol.* 167:149–160. http://dx.doi.org/10.1083/jcb.200402096

Haghikia, A., B. Stapel, M. Hoch, and D. Hilfiker-Kleiner. 2011. STAT3 and cardiac remodeling. *Heart Fail. Rev.* 16:35–47. http://dx.doi.org/10.1007/s10741-010-9170-x

Haghikia, A., M. Ricke-Hoch, B. Stapel, I. Gorst, and D. Hilfiker-Kleiner. 2014. STAT3, a key regulator of cell-to-cell communication in the heart. *Cardiovasc. Res.* 102:281–289. http://dx.doi.org/10.1093/cvr/cvu034

Hartlieb, E., V. Rötzer, M. Radeva, V. Spindler, and J. Waschke. 2014. Desmoglein 2 compensates for desmoglein 3 but does not control cell adhesion via regulation of p38 mitogen-activated protein kinase in keratinocytes. *J. Biol. Chem.* 289:17043–17053. http://dx.doi.org/10.1074/jbc.M113.489336

Hatzfeld, M. 2007. Plakophilins: Multifunctional proteins or just regulators of desmosomal adhesion? *Biochim. Biophys. Acta.* 1773:69–77. http://dx.doi.org/10.1016/j.bbamcr.2006.04.009

Jellis, C., J. Martin, J. Narula, and T.H. Marwick. 2010. Assessment of nonischemic myocardial fibrosis. *J. Am. Coll. Cardiol.* 56:89–97. http://dx.doi.org/10.1016/j.jacc.2010.02.047

Kim, S.I., J.H. Kwak, M. Zachariah, Y. He, L. Wang, and M.E. Choi. 2007. TGF-beta-activated kinase 1 and TAK1-binding protein 1 cooperate to mediate TGF-beta1-induced MKK3-p38 MAPK activation and stimulation of type I collagen. *Am. J. Physiol. Renal Physiol.* 292:F1471–F1478. http://dx.doi.org/10.1152/ajprenal.00485.2006

Kirchner, F., A. Schuetz, L.-H.H. Boldt, K. Martens, G. Dittmar, W. Haverkamp, L. Thierfelder, U. Heinemann, and B. Gerull. 2012. Molecular insights into arrhythmogenic right ventricular cardiomyopathy caused by plakophilin-2 missense mutations. *Circ Cardiovasc Genet.* 5:400–411. http://dx.doi.org/10.1161/CIRCGENETICS.111.961854

Klingberg, F., B. Hinz, and E.S. White. 2013. The myofibroblast matrix: implications for tissue repair and fibrosis. *J. Pathol.* 229:298–309. http://dx.doi.org/10.1002/path.4104

Krenning, G., E.M. Zeisberg, and R. Kalluri. 2010. The origin of fibroblasts and mechanism of cardiac fibrosis. *J. Cell. Physiol.* 225:631–637. http://dx.doi.org/10.1002/jcp.22322

Leask, A. 2007. TGFbeta, cardiac fibroblasts, and the fibrotic response. *Cardiovasc. Res.* 74:207–212. http://dx.doi.org/10.1016/j.cardiores.2006.07.012

Leask, A. 2010. Potential therapeutic targets for cardiac fibrosis: TGFbeta, angiotensin, endothelin, CCN2, and PDGF, partners in fibroblast activation. *Circ. Res.* 106:1675–1680. http://dx.doi.org/10.1161/CIRCRESAHA.110.217737

Leask, A., and D.J. Abraham. 2004. TGF-beta signaling and the fibrotic response. *FASEB J.* 18:816–827. http://dx.doi.org/10.1096/fj.03-1273rev

Li, J., D. Swope, N. Raess, L. Cheng, E.J. Muller, and G.L. Radice. 2011. Cardiac tissue-restricted deletion of plakoglobin results in progressive cardiomyopathy and activation of beta-catenin signaling. *Mol. Cell. Biol.* 31:1134–1144. http://dx.doi.org/10.1128/MCB.01025-10

Manabe, I., T. Shindo, and R. Nagai. 2002. Gene expression in fibroblasts and fibrosis: involvement in cardiac hypertrophy. *Circ. Res.* 91:1103–1113. http://dx.doi.org/10.1161/01.RES.0000046452.67724.B8

Massagué, J., J. Seoane, and D. Wotton. 2005. Smad transcription factors. *Genes Dev.* 19:2783–2810. http://dx.doi.org/10.1101/gad.1350705

Matsumoto-Ida, M., Y. Takimoto, T. Aoyama, M. Akao, T. Takeda, and T. Kita. 2006. Activation of TGF-beta1-TAK1-p38 MAPK pathway in spared cardiomyocytes is involved in left ventricular remodeling after myocardial infarction in rats. *Am. J. Physiol. Heart Circ. Physiol.* 290:H709–H715. http://dx.doi.org/10.1152/ajpheart.00186.2005

Moore, B.B., L. Murray, A. Das, C.A. Wilke, A.B. Herrygers, and G.B. Toews. 2006. The role of CCL12 in the recruitment of fibrocytes and lung fibrosis. *Am. J. Respir. Cell Mol. Biol.* 35:175–181. http://dx.doi.org/10.1165/rcmb.2005-0239OC

Munoz, W.A., M. Lee, R.K. Miller, Z. Ahmed, H. Ji, T.M. Link, G.R. Lee, M. Kloc, J.E. Ladbury, and P.D. McCrea. 2014. Plakophilin-3 catenin associates with the ETV1/ER81 transcription factor to positively modulate gene activity. *PLoS One.* 9:e86784. http://dx.doi.org/10.1371/journal.pone.0086784

Muraoka, N., H. Yamakawa, K. Miyamoto, T. Sadahiro, T. Umei, M. Isomi, H. Nakashima, M. Akiyama, R. Wada, K. Inagawa, et al. 2014. MiR-133 promotes cardiac reprogramming by directly repressing Snai1 and silencing fibroblast signatures. *EMBO J.* 33:1565–1581. http://dx.doi.org/10.15252/embj.201387605

Ono, K., T. Ohtomo, J. Ninomiya-Tsuji, and M. Tsuchiya. 2003. A dominant negative TAK1 inhibits cellular fibrotic responses induced by TGF-beta. *Biochem. Biophys. Res. Commun.* 307:332–337. http://dx.doi.org/10.1016/S0006-291X(03)01207-5

Oxford, E.M., H. Musa, K. Maass, W. Coombs, S.M. Taffet, and M. Delmar. 2007. Connexin43 remodeling caused by inhibition of plakophilin-2 expression in cardiac cells. *Circ. Res.* 101:703–711. http://dx.doi.org/10.1161/CIRCRESAHA.107.154252

Patel, D.M., A.D. Dubash, G. Kreitzer, and K.J. Green. 2014. Disease mutations in desmoplakin inhibit Cx43 membrane targeting mediated by desmoplakin-EB1 interactions. *J. Cell Biol.* 206:779–797. http://dx.doi.org/10.1083/jcb.201312110

Pearson, J.T., M.J. Jenkins, A.J. Edgley, T. Sonobe, M. Joshi, M.T. Waddingham, Y. Fujii, D.O. Schwenke, H. Tsuchimochi, M. Yoshimoto, et al. 2013. Acute Rho-kinase inhibition improves coronary dysfunction in vivo, in the early diabetic microcirculation. *Cardiovasc. Diabetol.* 12:111. http://dx.doi.org/10.1186/1475-2840-12-111

Pieperhoff, S., H. Schumacher, and W.W. Franke. 2008. The area composita of adhering junctions connecting heart muscle cells of vertebrates. V. The importance of plakophilin-2 demonstrated by small interference RNA-mediated knockdown in cultured rat cardiomyocytes. *Eur. J. Cell Biol.* 87:399–411. http://dx.doi.org/10.1016/j.ejcb.2007.12.002

Sato, P.Y., H. Musa, W. Coombs, G. Guerrero-Serna, G.A. Patiño, S.M. Taffet, L.L. Isom, and M. Delmar. 2009. Loss of plakophilin-2 expression leads to decreased sodium current and slower conduction velocity in cultured cardiac myocytes. *Circ. Res.* 105:523–526. http://dx.doi.org/10.1161/CIRCRESAHA.109.201418

Sato, P.Y., W. Coombs, X. Lin, O. Nekrasova, K.J. Green, L.L. Isom, S.M. Taffet, and M. Delmar. 2011. Interactions between ankyrin-G, Plakophilin-2, and Connexin43 at the cardiac intercalated disc. *Circ. Res.* 109:193–201. http://dx.doi.org/10.1161/CIRCRESAHA.111.247023

Siletz, A., M. Schnabel, E. Kniazeva, A.J. Schumacher, S. Shin, J.S. Jeruss, and L.D. Shea. 2013. Dynamic transcription factor networks in epithelial-mesenchymal transition in breast cancer models. *PLoS One.* 8:e57180. http://dx.doi.org/10.1371/journal.pone.0057180

Souders, C.A., S.L. Bowers, and T.A. Baudino. 2009. Cardiac fibroblast: the renaissance cell. *Circ. Res.* 105:1164–1176. http://dx.doi.org/10.1161/CIRCRESAHA.109.209809

Spindler, V., C. Dehner, S. Hübner, and J. Waschke. 2014. Plakoglobin but not desmoplakin regulates keratinocyte cohesion via modulation of p38MAPK signaling. *J. Invest. Dermatol.* 134:1655–1664. http://dx.doi.org/10.1038/jid.2014.21

Swope, D., L. Cheng, E. Gao, J. Li, and G.L. Radice. 2012. Loss of cadherin-binding proteins β-catenin and plakoglobin in the heart leads to gap junction remodeling and arrhythmogenesis. *Mol. Cell. Biol.* 32:1056–1067. http://dx.doi.org/10.1128/MCB.06188-11

Swope, D., J. Li, and G.L. Radice. 2013. Beyond cell adhesion: the role of armadillo proteins in the heart. *Cell. Signal.* 25:93–100. http://dx.doi.org/10.1016/j.cellsig.2012.09.025

Syrris, P., D. Ward, A. Asimaki, S. Sen-Chowdhry, H.Y. Ebrahim, A. Evans, N. Hitomi, M. Norman, A. Pantazis, A.L. Shaw, et al. 2006. Clinical expression of plakophilin-2 mutations in familial arrhythmogenic right ventricular cardiomyopathy. *Circulation.* 113:356–364. http://dx.doi.org/10.1161/CIRCULATIONAHA.105.561654

Takeishi, Y., Q. Huang, J. Abe, W. Che, J.-D.D. Lee, H. Kawakatsu, B.D. Hoit, B.C. Berk, and R.A. Walsh. 2002. Activation of mitogen-activated protein kinases and p90 ribosomal S6 kinase in failing human hearts with dilated cardiomyopathy. *Cardiovasc. Res.* 53:131–137. http://dx.doi.org/10.1016/S0008-6363(01)00438-2

Tenhunen, O., J. Rysä, M. Ilves, Y. Soini, H. Ruskoaho, and H. Leskinen. 2006. Identification of cell cycle regulatory and inflammatory genes as predominant targets of p38 mitogen-activated protein kinase in the heart. *Circ. Res.* 99:485–493. http://dx.doi.org/10.1161/01.RES.0000238387.85144.92

Todorović, V., B.V. Desai, M.J. Patterson, E.V. Amargo, A.D. Dubash, T. Yin, J.C. Jones, and K.J. Green. 2010. Plakoglobin regulates cell motility through Rho- and fibronectin-dependent Src signaling. *J. Cell Sci.* 123:3576–3586. http://dx.doi.org/10.1242/jcs.070391

Van Doren, S.R. 2015. Matrix metalloproteinase interactions with collagen and elastin. *Matrix Biol.* 44-46:224–231. http://dx.doi.org/10.1016/j.matbio.2015.01.005

Vasioukhin, V., L. Degenstein, B. Wise, and E. Fuchs. 1999. The magical touch: genome targeting in epidermal stem cells induced by tamoxifen application to mouse skin. *Proc. Natl. Acad. Sci. USA.* 96:8551–8556. http://dx.doi.org/10.1073/pnas.96.15.8551

Vasioukhin, V., E. Bowers, C. Bauer, L. Degenstein, and E. Fuchs. 2001. Desmoplakin is essential in epidermal sheet formation. *Nat. Cell Biol.* 3:1076–1085. http://dx.doi.org/10.1038/ncb1201-1076

Weber, K.T., Y. Sun, S.K. Bhattacharya, R.A. Ahokas, and I.C. Gerling. 2013. Myofibroblast-mediated mechanisms of pathological remodelling of the heart. *Nat. Rev. Cardiol.* 10:15–26. http://dx.doi.org/10.1038/nrcardio.2012.158

Wynn, T.A. 2008. Cellular and molecular mechanisms of fibrosis. *J. Pathol.* 214:199–210. http://dx.doi.org/10.1002/path.2277

Wynn, T.A., and T.R. Ramalingam. 2012. Mechanisms of fibrosis: therapeutic translation for fibrotic disease. *Nat. Med.* 18:1028–1040. http://dx.doi.org/10.1038/nm.2807

Yang, Z., N.E. Bowles, S.E. Scherer, M.D. Taylor, D.L. Kearney, S. Ge, V.V. Nadvoretskiy, G. DeFreitas, B. Carabello, L.I. Brandon, et al. 2006. Desmosomal dysfunction due to mutations in desmoplakin causes arrhythmogenic right ventricular dysplasia/cardiomyopathy. *Circ. Res.* 99:646–655. http://dx.doi.org/10.1161/01.RES.0000241482.19382.c6

Zhang, D., V. Gaussin, G.E. Taffet, N.S. Belaguli, M. Yamada, R.J. Schwartz, L.H. Michael, P.A. Overbeek, and M.D. Schneider. 2000. TAK1 is activated in the myocardium after pressure overload and is sufficient to provoke heart failure in transgenic mice. *Nat. Med.* 6:556–563. http://dx.doi.org/10.1038/75037